


**Emergence of composite many-body exciton states in WS<sub>2</sub> and MoSe<sub>2</sub> monolayers**J. Choi<sup>1,2</sup>, J. Li<sup>1,3</sup>, D. Van Tuan<sup>4</sup>, H. Dery<sup>4,5</sup> and S. A. Crooker<sup>1</sup><sup>1</sup>National High Magnetic Field Laboratory, Los Alamos, New Mexico 87545, USA<sup>2</sup>Advanced Instrumentation Institute, Korea Research Institute of Standards and Science, Daejeon 34113, Korea<sup>3</sup>Wuhan National High Magnetic Field Center and School of Physics, Huazhong University of Science and Technology, Hubei 430074, China<sup>4</sup>Department of Electrical and Computer Engineering, University of Rochester, Rochester, New York 14627, USA<sup>5</sup>Department of Physics and Astronomy, University of Rochester, Rochester, New York 14627, USA (Received 1 December 2023; revised 5 January 2024; accepted 10 January 2024; published 30 January 2024)

When doped with a high density of mobile charge carriers, monolayer transition-metal dichalcogenide (TMD) semiconductors can host new types of composite many-particle exciton states that do not exist in conventional semiconductors. Such multiparticle bound states arise when a photoexcited electron-hole pair couples not to just a single Fermi sea that is quantum-mechanically distinguishable (as in the case of conventional charged excitons or trions), but rather couples simultaneously to *multiple* Fermi seas, each having distinct spin and valley quantum numbers. Composite six-particle “hexciton” states were recently identified in electron-doped WSe<sub>2</sub> monolayers, but under suitable conditions they should also form in *all* other members of the monolayer TMD family. Here we present spectroscopic evidence demonstrating the emergence of many-body hexcitons in charge-tunable WS<sub>2</sub> monolayers (at the A-exciton) and MoSe<sub>2</sub> monolayers (at the B-exciton). The roles of distinguishability and carrier screening on the stability of hexcitons are discussed.

DOI: [10.1103/PhysRevB.109.L041304](https://doi.org/10.1103/PhysRevB.109.L041304)

Monolayer transition-metal dichalcogenide (TMD) semiconductors such as WSe<sub>2</sub>, MoSe<sub>2</sub>, WS<sub>2</sub>, and MoS<sub>2</sub> host a multitude of excitonic complexes due, in part, to the spin-orbit-split nature of their conduction and valence bands at the *K* and *K'* valleys of the Brillouin zone [1,2]. When they are optically allowed and possess a nonzero oscillator strength, these bound complexes manifest as discrete resonances in optical absorption spectra. Early studies of nominally undoped TMD monolayers revealed pronounced absorption peaks from the fundamental electron-hole optical transition (i.e., the  $X^0$  neutral exciton) [3–5]. Subsequent studies of charge-tunable TMD monolayers demonstrated the emergence, at lower energy, of additional strong absorption lines when the monolayers were populated with a background Fermi sea of holes or electrons (i.e., the  $X^\pm$  charged excitons) [6–8]. Whether, and under what conditions, a  $X^\pm$  complex is most accurately described as a simple three-particle “trion” (wherein the photoexcited exciton binds a carrier from the Fermi sea [6–11]) or a four-particle “tetron” (a trion additionally correlated with the resulting hole that is left behind in the Fermi sea [12–16]) or an “exciton-polaron” (an exciton dressed by collective excitations of the Fermi sea [17,18]) remains an active area of study and discussion [19–24].

Regardless of interpretation, all of these descriptions share a common understanding:  $X^\pm$  are bound states arising from the interaction of a photoexcited electron-hole (*e-h*) pair with the *subset* of carriers in the Fermi sea that have *distinguishable* quantum numbers. In most conventional III-V and II-IV semiconductors such as GaAs and ZnSe, where band extrema occur at the single central  $\Gamma$ -point valley of the Brillouin zone [9–11], this means that  $X^\pm$  forms with mobile carriers having opposite *spin* to that of the photoexcited electron or hole because Pauli exclusion prevents strong short-range

interactions with same-spin carriers. However, the multivalley nature of monolayer TMDs expands the basis set of available quantum numbers, and band-edge electrons and holes can be distinguished not only by their spin (up or down) but also by their valley degree of freedom (*K* or *K'*). TMD monolayers therefore permit, under suitable conditions, photoexcited *e-h* pairs to interact with Fermi seas containing *more than one* type of quantum-mechanically distinguishable carrier. As demonstrated recently [25–27], this leads to qualitatively new types of multiparticle composite exciton ground states that can be described as bound six-particle “hexcitons” (when photoexcited *e-h* pairs interact with two distinguishable Fermi seas) or even eight-particle “oxcitons” (when they interact with three distinguishable Fermi seas). These bound many-body excitonic states have large oscillator strengths and manifest as discrete absorption resonances in linear optical spectroscopy and emerge at energies even further below  $X^0$  and  $X^\pm$ . We emphasize that these composite hexcitons are optically allowed ground states of the interacting exciton–Fermi sea system and are therefore distinct from the many types of optically forbidden dark excitons and trions that appear only in photoluminescence studies [1,2,28–31] and, moreover, should not be confused with multiexciton complexes (such as biexcitons) that appear only at higher photoexcitation intensity [1,2,32–34].

To date, such multiparticle hexcitons have been identified and studied only in electron-doped WSe<sub>2</sub> monolayers [25–27]. This is due to (1) the excellent optical quality of exfoliated WSe<sub>2</sub>, (2) the ability to electrostatically dope WSe<sub>2</sub> to high electron densities, and (3) the fact that composite hexcitons in WSe<sub>2</sub> are expected at the low-energy A-exciton optical transitions where spectral linewidths are typically much sharper than at the higher-energy B-exciton. This latter

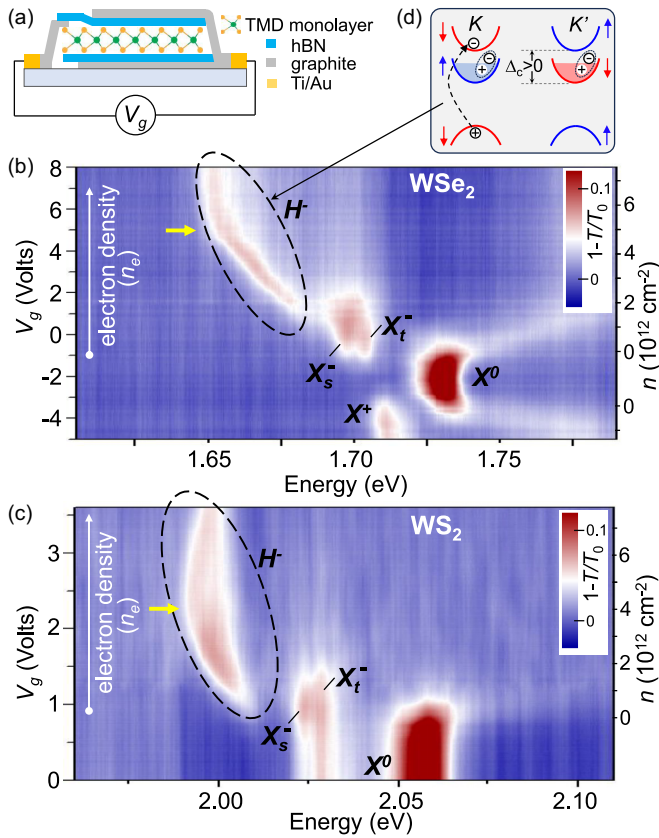


FIG. 1. (a) Schematic of the charge-tunable monolayer TMD structures. (b) and (c) Gate ( $V_g$ ) dependent optical absorption spectra at 4 K and  $B = 0$  from monolayer  $\text{WSe}_2$  and  $\text{WS}_2$ , respectively, at their A-exciton band edges. Similar to  $\text{WSe}_2$ ,  $\text{WS}_2$  exhibits strong  $X^0$  absorption at charge neutrality, conventional  $X_{s,t}^\pm$  absorption at small electron density  $n_e$ , and, at even lower energy, the emergence of a strong “hexciton” absorption resonance at larger  $n_e$  (dashed oval, labeled  $H^-$ ). (d) Band diagram of  $\text{WSe}_2$  and  $\text{WS}_2$ . Extending the picture of  $X^\pm$  as four-particle tetrons, the hexciton corresponds to a six-particle correlated state that forms when a photoexcited  $e$ - $h$  pair couples simultaneously to *both* of the quantum-mechanically distinguishable Fermi seas residing in the two lower CBs. This occurs in  $\text{WSe}_2$  and  $\text{WS}_2$  at the A-exciton because  $\Delta_c > 0$ , such that optical transitions promote electrons to the upper CBs, where they are distinguishable from electrons in the Fermi sea. Blue (red) denotes spin-up (spin-down) bands. For clarity, only optical transitions in the  $K$  valley are depicted. The redshift of the hexciton ceases (yellow arrows) when the Fermi sea begins to fill the upper CBs, which is at  $n_e \approx 5 \times 10^{12} \text{ cm}^{-2}$  ( $4 \times 10^{12} \text{ cm}^{-2}$ ) for  $\text{WSe}_2$  ( $\text{WS}_2$ ).

fact arises from the positive sign of the conduction band (CB) spin-orbit splitting in  $\text{WSe}_2$  ( $\Delta_c > 0$ ) [35,36], which mandates that A-exciton optical transitions photoexcite electrons to the *upper* CBs in  $K$  and  $K'$ , where Pauli exclusion does not prevent them from interacting with *both* of the distinguishable Fermi seas of electrons that occupy the two lower CBs (as depicted in the band diagram in Fig. 1, one Fermi sea resides in the same valley but has opposite spin; the other has the same spin but resides in the opposite valley).

However, under appropriate conditions, composite hexcitons should also emerge in *all* members of the monolayer TMD family. For example, monolayer  $\text{WS}_2$  also has a pos-

itive  $\Delta_c$  and CB structure similar to  $\text{WSe}_2$ , and therefore, hexcitons should also appear at its A-exciton under conditions of high electron doping. In contrast, the negative  $\Delta_c$  of monolayer  $\text{MoSe}_2$  [35,36] precludes the existence of hexcitons at its A-exciton (instead, only conventional  $X^\pm$  should appear) but *does* allow for the formation of hexcitons at its B-exciton transition. To date, neither of these predictions has been explicitly tested. Here, using low-temperature optical absorption measurements of electrostatically gated  $\text{WS}_2$  and  $\text{MoSe}_2$  monolayers, we demonstrate and investigate the emergence of composite hexcitons in both  $\text{WS}_2$  monolayers (at the A-exciton) and  $\text{MoSe}_2$  monolayers (at the B-exciton). Based on the data, the influences of distinguishability and carrier screening on the stability of hexcitons are discussed.

Figure 1(a) depicts the charge-tunable TMD monolayer samples studied in this work. Single-monolayer flakes of  $\text{WS}_2$ ,  $\text{MoSe}_2$ , and  $\text{WSe}_2$  were mechanically exfoliated and sandwiched between thin slabs of insulating hexagonal boron nitride (hBN; typically, 15–25 nm thick,  $\epsilon_{\text{hBN}} = 3$ ). Few-layer graphite flakes were used to electrically contact the monolayers and to serve as top and bottom gates. In this work, the top and bottom gates were tied together, and gate voltage  $V_g$  was used to electrostatically dope the monolayers with a background Fermi sea of electrons or holes. Dual gating allows us to attain high carrier densities approaching  $10^{13}/\text{cm}^2$ . Each assembled structure was then positioned and placed directly over the core of a single-mode optical fiber to ensure a rigid and robust alignment between the optical path and the doped TMD monolayer. This approach [37,38] mitigates the drift and vibration that can otherwise complicate optical studies of TMD monolayers at low temperatures and in the pulsed magnetic fields used in this work.

The sample-on-fiber assembly was then mounted on a purpose-built probe and loaded into a liquid helium cryostat. Broadband white light from a xenon lamp was directed down the single-mode fiber. Following transmission through the sample, the light passed through a thin-film circular polarizer and was then retroreflected and directed back into a multi-mode collection fiber. The transmitted light was dispersed in a 300 mm spectrometer and detected by a charge-coupled device. In this way the optical absorption from the doped TMD monolayer was directly measured as  $1 - T/T_0$ , where  $T$  is the spectrum of the transmitted light and  $T_0$  is a reference spectrum. We note that absorption spectra typically permit a straightforward evaluation and visualization of exciton oscillator strengths, in contrast to reflectivity studies where line shapes depend sensitively on interference effects from the surrounding layer structure.

Figure 1(b) shows a map of the gate-dependent absorption spectra from a  $\text{WSe}_2$  monolayer at low temperature (4 K) and at zero magnetic field in the spectral range of its A-exciton. When  $V_g \approx -2\text{V}$ , the monolayer is at its charge neutrality point, and only the neutral exciton ( $X^0$ ) absorption resonance is observed. At increasingly negative or positive  $V_g$ , the monolayer becomes lightly doped with mobile holes or electrons, and the well-known  $X^\pm$  resonances appear at energies  $\approx 20$ – $35$  meV below  $X^0$ . As extensively described in previous works,  $X^\pm$  are optically active bound states arising from the interaction of the photoexcited  $e$ - $h$  pair with the carriers in the Fermi sea that possess quantum numbers that

are distinguishable from those of the photoexcited  $e$ - $h$  pair (i.e., different spin and/or valley). Thus, only a single  $X^+$  resonance appears on the hole-doped side, but two conventional  $X^-$  resonances appear on the electron-doped side (the so-called singlet  $X_s^-$  and triplet  $X_t^-$  charged excitons) because there are two distinct Fermi seas with which to interact. The different energies of  $X_s^-$  and  $X_t^-$  stem from the different amplitude of the short-range electron-hole exchange interaction [20,39,40].

Most importantly, at higher  $n_e$  the  $X_s^-$  and  $X_t^-$  resonances disappear, and a new strong absorption resonance appears at even lower energy ( $\approx 15$  meV below  $X_s^-$ ), indicating the emergence of a new bound excitonic ground state with large oscillator strength. First observed in gated WSe<sub>2</sub> monolayers in 2013 [41] and very clearly resolved in several subsequent studies [8,24,32,42,43], this low-energy absorption resonance—occasionally called  $X^{-'}$  in earlier studies—completely dominates the absorption spectrum of WSe<sub>2</sub> at high  $n_e$ . Moreover, it does not appear in hole-doped WSe<sub>2</sub> at the A-exciton and does not appear in the A-exciton absorption spectrum of gated MoSe<sub>2</sub> monolayers [8,44]. Recently, this absorption resonance was identified as a qualitatively new type of many-body composite (six-particle hexciton) state, arising from the simultaneous interaction of the photoexcited  $e$ - $h$  pair with *both* of the Fermi seas that reside in the lower CBs of monolayer WSe<sub>2</sub> [25–27]. As depicted in Fig. 1(d), each of these two Fermi seas has quantum numbers that are distinguishable from those of the photoexcited electron (one has opposite spin; the other has opposite valley). Extending the picture of  $X^\pm$  being four-particle tetrons [14,16], the hexciton bound state comprises the photoexcited  $e$ - $h$  pair, an electron from each of the two distinguishable Fermi seas, and the two Fermi holes that are left behind in the Fermi seas. As described recently, hexcitons are the stable ground state of this interacting exciton-Fermi sea system, and the Fermi holes not only ensure overall charge neutrality but also provide the “glue” that binds the complex [26,27].

The ordering of the spin- and valley-polarized CBs in monolayer WS<sub>2</sub> is similar to that of WSe<sub>2</sub> (i.e.,  $\Delta_c$  is also positive), and optical transitions at the A-exciton couple to the upper CBs. Consequently, optical signatures of composite hexcitons can therefore be anticipated at high  $n_e$  in WS<sub>2</sub> monolayers. The gate-dependent absorption map of Fig. 1(c) confirms this prediction: Strong absorption from  $X^0$  is plainly visible at  $V_g \approx 0$ , and  $X_{s,t}^-$  charged excitons appear at low  $n_e$ . These conventional  $X_{s,t}^-$  resonances in WS<sub>2</sub> were clearly resolved in several recent studies [45–48]. Most importantly, our dual-gated structure allows a smooth tuning to a regime of high  $n_e$ , where Fig. 1(c) shows that  $X_{s,t}^-$  disappear and a new strong absorption resonance emerges at even lower energy ( $\approx 15$  meV below  $X_s^-$ ). The gate-dependent absorption of monolayer WS<sub>2</sub> is therefore qualitatively identical to that of WSe<sub>2</sub>, albeit with broader linewidths that are likely due to the reduced material quality of sulfur-based TMDs. Thus, we associate the emergence of the low-energy absorption resonance with the stable formation of six-particle hexciton states. Note that we were unable to dope our WS<sub>2</sub> monolayers with mobile holes; even at large negative  $V_g$ , only the neutral  $X_0$  exciton was visible, likely due to strong mid-gap pinning of the Fermi level by the larger number of defects in sulfur-based TMDs.

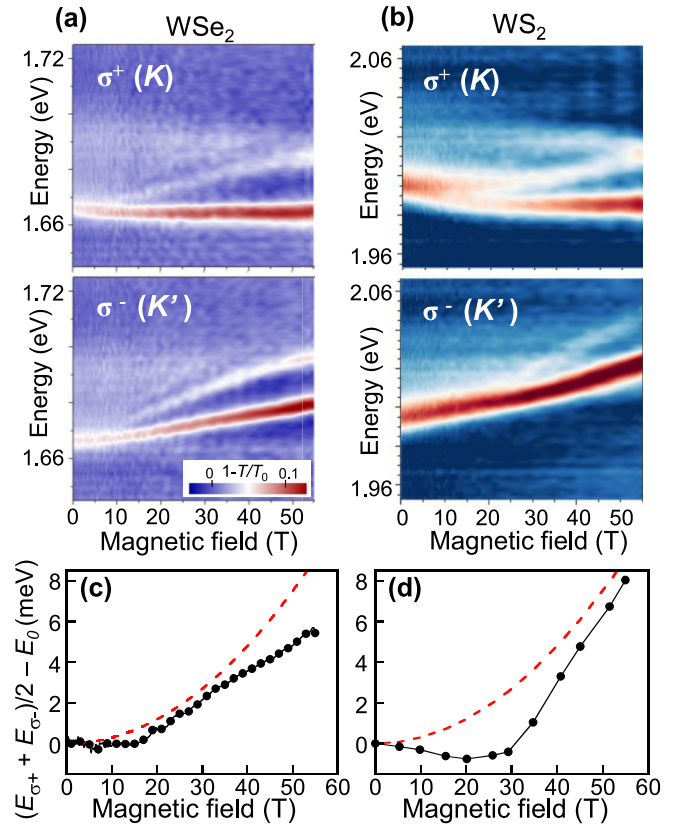


FIG. 2. (a) and (b) Magnetic field evolution of the hexciton absorption resonance in monolayer WSe<sub>2</sub> and WS<sub>2</sub>, respectively, for both  $\sigma^+$  and  $\sigma^-$  circularly polarized light, showing clear valley Zeeman splitting and the appearance of higher-energy absorption lines corresponding to optical transitions to higher Landau levels ( $V_g = 2$  V). (c) and (d) The *average* energy of the  $\sigma^+$  and  $\sigma^-$  absorption lines reveals the diamagnetic shift of the hexciton absorption resonance, which does not follow a purely quadratic dependence (even at low  $B$ ). As a point of reference, the dashed red curves depict a  $\sigma B^2$  shift, using a diamagnetic coefficient  $\sigma = 3 \mu\text{eV}/\text{T}^2$ , which is  $\approx 10$  times larger than the small diamagnetic shifts of the neutral exciton in WSe<sub>2</sub> and WS<sub>2</sub>.

Additional evidence supporting a picture of hexcitons in monolayer WS<sub>2</sub> is the evolution of its optical resonance in applied magnetic fields  $B$ . Figure 2 shows circularly polarized magnetoabsorption from both WSe<sub>2</sub> and WS<sub>2</sub> under conditions of large  $n_e$ , where the hexciton absorption dominates. As shown recently [25], the hexciton resonance in WSe<sub>2</sub> monolayers splits and shifts with increasing  $B$ , and additional absorption resonances appear at higher energy that disperse linearly with  $B$  and are related to the development of Landau levels (LLs) in the conduction and valence bands. Figure 2 shows that a qualitatively similar  $B$ -dependent evolution of the hexciton peak also exists in WS<sub>2</sub>, where additional LL-like absorption features emerge for  $B > 30$  T. From the separation of these peaks we can estimate a combined electron and hole cyclotron resonance energy of  $\approx 0.45$  meV/T, which is slightly larger than that obtained from WSe<sub>2</sub> [25] but in line with expectation given the slightly lighter carrier masses in WS<sub>2</sub> [49].

Moreover, from these spectra we can extract the diamagnetic shifts of the hexciton resonance, given by the *average* of the  $\sigma^+$  and  $\sigma^-$  absorption energies. This analysis, shown in Figs. 2(c) and 2(d), reveals that the diamagnetic shifts of hexcitons, even at low  $B$ , deviate from the purely quadratic behavior that is known to exist for neutral excitons in WSe<sub>2</sub> and WS<sub>2</sub> [37,49] (especially for WS<sub>2</sub>, where atypical diamagnetic shifts have also been observed for charged excitons [50]). This behavior may arise from nonzero angular momentum contributions from the particles in the hexciton complex and will be further investigated in future studies. For reference, however, the dotted red curves depict purely quadratic shifts ( $\sigma B^2$ ) using a large diamagnetic coefficient  $\sigma = 3 \mu\text{eV}/\text{T}^2$ , which is 10 times larger than the known diamagnetic shifts of the very small and tightly bound neutral excitons [37,49]. To the extent that these curves approximately capture the overall shifts of the hexciton resonances, these data are qualitatively consistent with recent calculations indicating that composite hexcitons are several times larger in size than neutral excitons [26,27]

Taken together, these data provide evidence of the emergence of composite hexciton states in electron-doped monolayer WS<sub>2</sub>, which appear at the A-exciton owing to the positive sign of  $\Delta_c$  and consequent ordering of the spin-orbit-split CBs in the  $K$  and  $K'$  valleys.

In marked contrast, neither electron-doped nor hole-doped MoSe<sub>2</sub> monolayers show any indication of hexciton formation at the A-exciton, as shown in Fig. 3(a). Rather, as observed in earlier studies [8,24,44], charge-tunable MoSe<sub>2</sub> monolayers exhibit only a single  $X^-$  and  $X^+$  absorption that appears  $\approx 25$  meV below the neutral exciton  $X_A^0$ . This observation is consistent with the negative sign of  $\Delta_c$  in MoSe<sub>2</sub> [35,36], which dictates that optical transitions at the A-exciton photoexcite electrons to the lower (not upper) CBs. As such, when mobile electrons populate the lower CBs, only a single type of distinguishable electron exists in the Fermi sea, and many-body hexcitons cannot form [see diagrams in Figs. 3(b) and 3(d)].

The ordering of the CBs in MoSe<sub>2</sub> *does*, however, permit hexciton formation at the higher-energy B-exciton, where optical transitions couple to the upper CBs [see Fig. 3(c)]. As Fig. 3(a) shows, when  $n_e$  is small, the neutral B-exciton  $X_B^0$  at 1.84 eV disappears, and only a faint and diffuse absorption remains at energies where conventional charged excitons are expected (that is, at about 25 meV below  $X_B^0$ , or  $\approx 1.815$  eV). However, at larger  $n_e$  ( $\approx 5 \times 10^{12} \text{ cm}^{-2}$ ), a stronger absorption with increased oscillator strength clearly emerges at  $\approx 1.795$  eV. Its separation from  $X_B^0$  is  $\approx 45$  meV, which is larger than the 25 meV expected for conventional charged excitons but is commensurate with the larger energy separation between hexcitons and neutral excitons that we observed in WSe<sub>2</sub> and WS<sub>2</sub> (see Fig. 1). Notably, Fig. 3 shows that this new absorption does not emerge *until* a large  $n_e$  comparable to where the conventional  $X^-$  trion loses oscillator strength, suggesting that it is not a conventional trion. Therefore, although past studies of charge-tunable MoSe<sub>2</sub> monolayers have associated similar spectral signatures with conventional trions, tetrons, and exciton-polarons of the B-exciton [8,24], we argue that the low energy of the emerging absorption resonance and (especially) its dependence on  $n_e$

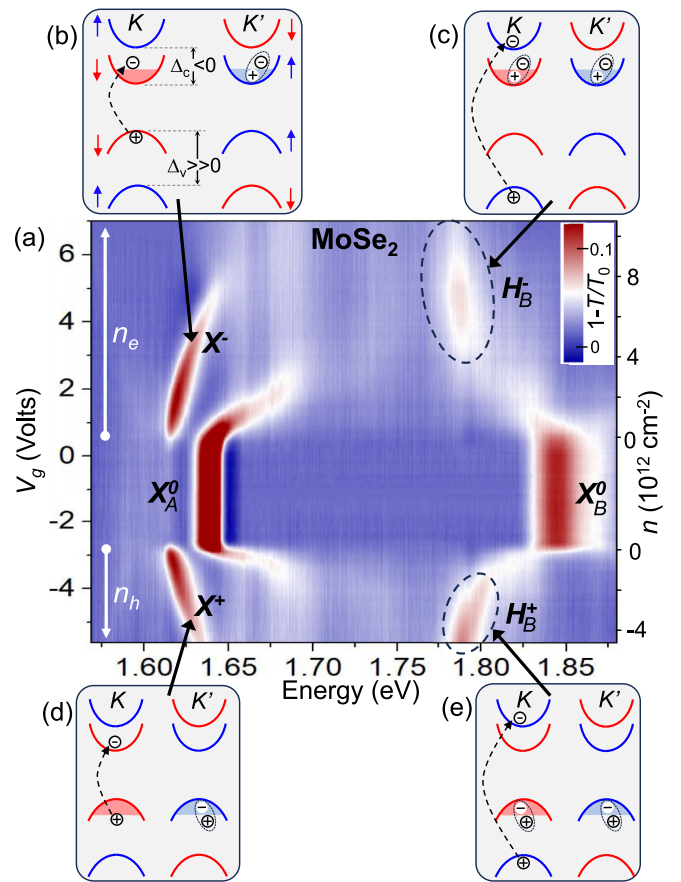


FIG. 3. (a) Gate-dependent absorption of a charge-tunable MoSe<sub>2</sub> monolayer at 4 K. Only conventional  $X^-$  and  $X^+$  are observed at the A-exciton ( $\sim 1.63$  eV), even at large electron or hole densities, because  $\Delta_c < 0$  and therefore only a single distinguishable Fermi sea is available; see the diagrams in (b) and (d), respectively. But at the B-exciton ( $\sim 1.83$  eV), photoexcited  $e$ - $h$  pairs couple to the upper CBs, and interaction with both Fermi seas in the lower CBs is possible, leading to hexciton formation at higher  $n_e$ ; see the diagram in (c). Moreover, hexciton formation at high hole densities is always possible at the B-exciton (for *all* TMD monolayers because  $\Delta_v \gg 0$ ); see the diagram in (e). Blue (red) in the diagrams denotes spin-up (spin-down) bands. For clarity, only optical transitions in the  $K$  valley are depicted.

are, in fact, more consistent with the formation and emergence of many-body hexcitons in electron-doped MoSe<sub>2</sub> monolayers.

Furthermore, analogous signatures of hexcitons appear when the MoSe<sub>2</sub> monolayer is doped with high concentrations of mobile holes  $n_h$  [see Fig. 3(a)]. As depicted in the diagram in Fig. 3(e),  $e$ - $h$  pairs excited at the B-exciton will *always* have two distinguishable Fermi seas of mobile holes with which to interact, and composite hexcitons can be anticipated. Figure 3(a) shows that as  $n_h$  starts to increase, both  $X_A^0$  and  $X_B^0$  disappear, and a conventional  $X^+$  resonance appears 25 meV below  $X_A^0$  when  $V_g = -3$  V. However, the concomitant response at the B-exciton is much weaker, until  $V_g$  increases up to  $\approx -4$  V, at which point a strong absorption emerges at a much lower energy of  $\approx 40$  meV below  $X_B^0$ . This new resonance actually *gains* oscillator strength with increasing

$n_h$ , while in this same doping range the conventional  $X^+$  fades away. Based on this  $n_h$  dependence, we rule out the possibility that the new resonance could be, e.g., a conventional trion associated with  $X_B^0$  or an excited Rydberg state of  $X_A^0$ . Moreover, this new resonance redshifts with increasing  $n_h$ , similar to the redshift observed for hexcitons in electron-doped  $\text{WSe}_2$  and  $\text{WS}_2$  (see Fig. 1). These data therefore support a picture of robust hexciton formation at the B-exciton in hole-doped  $\text{MoSe}_2$ . The resonance features are rather broad, however, likely due to the shorter lifetime of B-excitons.

Indeed, owing to the large (hundreds of meV) spin-orbit splitting of the valence bands  $\Delta_v$  that exists in all monolayer TMD semiconductors, robust hexciton formation at the B-exciton should emerge when *any* TMD monolayer semiconductor is doped with a high density of mobile holes [see diagram in Fig. 3(e)]. Furthermore, because  $\Delta_v$  is large, the Fermi sea of holes never occupies the valence bands from which the photoexcited  $e$ - $h$  pair originates, and the photohole always remains distinguishable from every hole in the Fermi sea. Hexcitons under such conditions should therefore remain robust and should redshift due to the primary effects of band gap renormalization [51] up to very large values of  $n_h$ . While in this work we have studied B-excitons only in  $\text{MoSe}_2$ , we note that the seminal work of Wang *et al.* [8] clearly revealed a strong absorption below  $X_B^0$  in heavily hole-doped  $\text{WSe}_2$  monolayers that redshifted with increasing  $n_h$  and did not broaden, consistent with hexciton formation.

An important insight gained from these various results is that the decay and broadening of excitonic complexes are likely governed more by the quantum-mechanical distinguishability of the photoexcited  $e$ - $h$  pair (in relation to the carriers in the Fermi sea) than by screening from the Fermi sea. For example, in the case of electron-doped  $\text{WSe}_2$  and  $\text{WS}_2$  shown in Fig. 1, the redshifts of the hexciton resonances in  $\text{WSe}_2$  and  $\text{WS}_2$  cease, and their decay or broadening begins only when electrons begin to populate the upper CBs. Beyond this point, the photoexcited electron is no longer distinguishable from every electron in the Fermi sea, and the Pauli exclusion principle dictates that when it is introduced into the (now occupied) upper CB, it must scatter away those mobile electrons having similar spin and valley quantum numbers [27]. This exchange scattering process leads to the decay and broadening of the hexciton resonance. Hexciton resonances therefore retain their amplitude and narrow linewidth when the charge density increases, as long as the photoexcited  $e$ - $h$  pair remains distinguishable from all carriers in the Fermi sea. In hole-doped TMD monolayers, the large  $\Delta_v$  ensures distinguishability of  $e$ - $h$  pairs excited at the B-exciton and therefore a robust stability of hexcitons even to very large  $n_h$ .

Moreover, screening by mobile carriers does not seem to be the primary driving force for broadening of the hexciton resonance, as inferred by the observation that the

conventional  $X^\pm$  resonances begin to lose oscillator strength at much smaller carrier density. For example, Fig. 3 shows that the conventional trions of  $\text{MoSe}_2$  around 1.63 eV decay when  $|V_g| \gtrsim 5$  V. Concomitantly, however, the type-B hexciton in hole-doped conditions around 1.8 eV neither broadens nor decays at the same (and even higher)  $n_h$ . A similar behavior was also measured for a wider  $n_h$  range by Liu *et al.* [24], where the type-B resonance around 1.8 eV maintains a large oscillator strength and continues to redshift long after the  $X^+$  resonance at the A-exciton decays. This suggests that screening is not the primary cause of decay and broadening because the Coulomb potential cannot selectively weaken the attraction between particles of one complex species but not of another.

In summary, composite hexcitons are expected in *all* members of the monolayer TMD family. When doped with a high density of electrons, hexcitons can emerge at the A-exciton resonance (like in the case of  $\text{WSe}_2$  and  $\text{WS}_2$ ) or the B-exciton resonance (like in the case of  $\text{MoSe}_2$ ) depending on the sign of  $\Delta_c$  and the consequent ordering of the CBs. For hole-doped TMD monolayers, hexcitons should *always* emerge at the B-exciton, as investigated here for  $\text{MoSe}_2$  and as suggested by earlier spectroscopic data from both  $\text{WSe}_2$  and  $\text{MoSe}_2$  [8,24]. To the best of our knowledge, this has not yet been studied in hole-doped  $\text{WS}_2$  or  $\text{MoS}_2$ . As a final point of discussion, we note that electron-doped  $\text{MoS}_2$  monolayers represent an interesting case: While early theory suggested that  $\Delta_c$  was small and negative (implying a CB ordering similar to  $\text{MoSe}_2$  [36]), more recent experimental work indicated an opposite CB ordering [52,53], particularly when exciton effects are taken into account, making it more akin to that of  $\text{WS}_2$  and  $\text{WSe}_2$ . In this case, a hexciton resonance can be expected to emerge in electron-doped  $\text{MoS}_2$  at the A-exciton, at an energy below that of the conventional  $X_{s,t}^\pm$  charged excitons. Indeed, various recent studies have revealed additional optical resonances emerging in electron-doped  $\text{MoS}_2$  monolayers [54–56], although in some cases they were associated with exotic ferromagnetic order. Looking forward, we anticipate that composite six-particle hexcitons (and, in high magnetic fields, eight-particle excitons) will provide a rich platform to study novel many-body effects and intervalley correlations within a strongly interacting exciton-Fermi sea system.

We thank Xavier Marie for helpful discussions, and we acknowledge support from the Los Alamos LDRD program and the U.S. Department of Energy (DOE) “Science of 100 T” program. The National High Magnetic Field Lab is supported by National Science Foundation Grant No. DMR-1644779, the state of Florida, and the U.S. DOE. Work at the University of Rochester was supported by the DOE Basic Energy Sciences, Division of Materials Sciences and Engineering, under Award No. DE-SC0014349.

[1] G. Wang, A. Chernikov, M. M. Glazov, T. F. Heinz, X. Marie, T. Amand, and B. Urbaszek, Excitons in atomically thin transition metal dichalcogenides, *Rev. Mod. Phys.* **90**, 021001 (2018).

[2] T. Mueller and E. Malic, Exciton physics and device application of two-dimensional transition metal dichalcogenide semiconductors, *npj 2D Mater.* **2**, 29 (2018).

- [3] A. Splendiani, L. Sun, Y. Zhang, T. Li, J. Kim, C.-Y. Chim, G. Galli, and F. Wang, Emerging photoluminescence in monolayer MoS<sub>2</sub>, *Nano Lett.* **10**, 1271 (2010).
- [4] K. F. Mak, C. Lee, J. Hone, J. Shan, and T. F. Heinz, Atomically thin MoS<sub>2</sub>: A new direct-gap semiconductor, *Phys. Rev. Lett.* **105**, 136805 (2010).
- [5] Y. Li, A. Chernikov, X. Zhang, A. Rigosi, H. M. Hill, A. M. van der Zande, D. A. Chenet, E.-M. Shih, J. Hone, and T. F. Heinz, Measurement of the optical dielectric function of monolayer transition-metal dichalcogenides: MoS<sub>2</sub>, MoSe<sub>2</sub>, WS<sub>2</sub>, and WSe<sub>2</sub>, *Phys. Rev. B* **90**, 205422 (2014).
- [6] J. S. Ross, S. Wu, H. Yu, N. J. Ghimire, A. M. Jones, G. Aivazian, J. Yan, D. G. Mandrus, D. Xiao, W. Yao, and X. Xu, Electrical control of neutral and charged excitons in a monolayer semiconductor, *Nat. Commun.* **4**, 1474 (2013).
- [7] K. F. Mak, K. He, C. Lee, G. H. Lee, J. Hone, T. F. Heinz, and J. Shan, Tightly bound trions in monolayer MoS<sub>2</sub>, *Nat. Mater.* **12**, 207 (2013).
- [8] Z. Wang, L. Zhao, K. F. Mak, and J. Shan, Probing the spin-polarized electronic band structure in monolayer transition metal dichalcogenides by optical spectroscopy, *Nano Lett.* **17**, 740 (2017).
- [9] K. Kheng, R. T. Cox, Merle Y. d'Aubigne, F. Bassani, K. Saminadayar, and S. Tatarenko, Observation of negatively charged excitons  $X^-$  in semiconductor quantum wells, *Phys. Rev. Lett.* **71**, 1752 (1993).
- [10] G. V. Astakhov, D. R. Yakovlev, V. P. Kochereshko, W. Ossau, W. Faschinger, J. Puls, F. Henneberger, S. A. Crooker, Q. McCulloch, D. Wolverson, N. A. Gippius, and A. Waag, Binding energy of charged excitons in ZnSe-based quantum wells, *Phys. Rev. B* **65**, 165335 (2002).
- [11] I. Bar-Joseph, Trions in GaAs quantum wells, *Semicond. Sci. Technol.* **20**, R29-R39 (2005).
- [12] F. X. Bronold, Absorption spectrum of a weakly  $n$ -doped semiconductor quantum well, *Phys. Rev. B* **61**, 12620 (2000).
- [13] R. A. Suris, V. P. Kochereshko, G. V. Astakhov, D. R. Yakovlev, W. Ossau, J. Nürnberger, W. Faschinger, G. Landwehr, T. Wojtowicz, G. Karczewski, and J. Kossut, Excitons and trions modified by interactions with a two-dimensional electron gas, *Phys. Stat. Sol. B* **227**, 343 (2001).
- [14] R. A. Suris, Correlation between trion and hole in Fermi distribution in process of trion photo-excitation in doped QWs, in *Optical Properties of 2D Systems with Interacting Electrons*, edited by W. Ossau and R. Suris, NATO Science Series, II: Mathematics, Physics and Chemistry Vol. 119 (Kluwer, Dordrecht, 2003), pp. 111–124.
- [15] Y.-C. Chang, S.-Y. Shiau, and M. Combescot, Crossover from trion-hole complex to exciton-polaron in  $n$ -doped two-dimensional semiconductor quantum wells, *Phys. Rev. B* **98**, 235203 (2018).
- [16] F. Rana, O. Koksai, C. Manolatu, Many-body theory of the optical conductivity of excitons and trions in two-dimensional materials, *Phys. Rev. B* **102**, 085304 (2020).
- [17] M. Sidler, P. Back, O. Cotlet, A. Srivastava, T. Fink, M. Kroner, E. Demler, and A. Imamoglu, Fermi polaron-polaritons in charge-tunable atomically thin semiconductors, *Nat. Phys.* **13**, 255 (2017).
- [18] D. K. Efimkin and A. H. MacDonald, Many-body theory of trion absorption features in two-dimensional semiconductors, *Phys. Rev. B* **95**, 035417 (2017).
- [19] Y.-W. Chang and D. R. Reichman, Many-body theory of optical absorption in doped two-dimensional semiconductors, *Phys. Rev. B* **99**, 125421 (2019).
- [20] M. M. Glazov, Optical properties of charged excitons in two-dimensional semiconductors, *J. Chem. Phys.* **153**, 034703 (2020).
- [21] F. Rana, O. Koksai, M. Jung, G. Shvets, A. N. Vamivakas, and C. Manolatu, Exciton-trion polaritons in doped two-dimensional semiconductors, *Phys. Rev. Lett.* **126**, 127402 (2021).
- [22] D. K. Efimkin, E. K. Laird, J. Levinsen, M. M. Parish, and A. H. MacDonald, Electron-exciton interactions in the exciton-polaron problem, *Phys. Rev. B* **103**, 075417 (2021).
- [23] C. Fey, P. Schmelcher, A. Imamoglu, and R. Schmidt, Theory of exciton-electron scattering in atomically thin semiconductors, *Phys. Rev. B* **101**, 195417 (2020).
- [24] E. Liu, J. van Baren, Z. Lu, T. Taniguchi, K. Watanabe, D. Smirnov, Y.-C. Chang, and C. H. Lui, Exciton-polaron Rydberg states in monolayer MoSe<sub>2</sub> and WSe<sub>2</sub>, *Nat. Commun.* **12**, 6131 (2021).
- [25] J. Li, M. Goryca, J. Choi, X. Xu, and S. A. Crooker, Many-body exciton and intervalley correlations in heavily electron-doped WSe<sub>2</sub> monolayers, *Nano Lett.* **22**, 426 (2022).
- [26] D. Van Tuan, S. F. Shi, X. Xu, S. A. Crooker, and H. Dery, Six-body and eight-body exciton states in monolayer WSe<sub>2</sub>, *Phys. Rev. Lett.* **129**, 076801 (2022).
- [27] D. Van Tuan and H. Dery, Composite excitonic states in doped semiconductors, *Phys. Rev. B* **106**, L081301 (2022).
- [28] C. Robert, T. Amand, F. Cadiz, D. Lagarde, E. Courtade, M. Manca, T. Taniguchi, K. Watanabe, B. Urbaszek, and X. Marie, Fine structure and lifetime of dark excitons in transition metal dichalcogenide monolayers, *Phys. Rev. B* **96**, 155423 (2017).
- [29] E. Malic, M. Selig, M. Feierabend, S. Brem, D. Christiansen, F. Wendler, A. Knorr, and G. Berghäuser, Dark excitons in transition metal dichalcogenides, *Phys. Rev. Mater.* **2**, 014002 (2018).
- [30] M. He, P. Rivera, D. V. Tuan, N. P. Wilson, M. Yang, T. Taniguchi, K. Watanabe, J. Yan, D. G. Mandrus, H. Yu, H. Dery, W. Yao, and X. Xu, Valley phonons and exciton complexes in a monolayer semiconductor, *Nat. Commun.* **11**, 618 (2020).
- [31] M. Yang, L. Ren, C. Robert, D. Van Tuan, L. Lombez, B. Urbaszek, X. Marie, and H. Dery, Relaxation and darkening of excitonic complexes in electrostatically doped monolayer WSe<sub>2</sub>: Roles of exciton-electron and trion-electron interactions, *Phys. Rev. B* **105**, 085302 (2022).
- [32] M. Barbone, A. R.-P. Montblanch, D. M. Kara, C. Palacios-Berraquero, A. R. Cadore, D. De Fazio, B. Pingault, E. Mostaani, H. Li, B. Chen, K. Watanabe, T. Taniguchi, S. Tongay, G. Wang, A. C. Ferrari, and M. Atature, Charge-tunable biexciton complexes in monolayer WSe<sub>2</sub>, *Nat. Commun.* **9**, 3721 (2018).
- [33] Z. Li, T. Wang, Z. Lu, C. Jin, Y. Chen, Y. Meng, Z. Lian, T. Taniguchi, K. Watanabe, S. Zhang, D. Smirnov, and S.-F. Shi, Revealing the biexciton and trion-exciton complexes in BN encapsulated WSe<sub>2</sub>, *Nat. Commun.* **9**, 3719 (2018).
- [34] S.-Y. Chen, T. Goldstein, T. Taniguchi, K. Watanabe, and J. Yan, Coulomb-bound four- and five-particle intervalley states in an atomically-thin semiconductor, *Nat. Commun.* **9**, 3717 (2018).

- [35] Y. Song and H. Dery, Transport theory of monolayer transition-metal dichalcogenides through symmetry, *Phys. Rev. Lett.* **111**, 026601 (2013).
- [36] A. Kormányos, G. Burkard, M. Gmitra, J. Fabian, V. Zólyomi, N. D. Drummond, and V. Fal'ko,  $\mathbf{k}, \mathbf{p}$  theory for two-dimensional transition metal dichalcogenide semiconductors, *2D Mater.* **2**, 022001 (2015).
- [37] A. V. Stier, N. P. Wilson, K. A. Velizhanin, J. Kono, X. Xu, and S. A. Crooker, Magneto-optics of exciton Rydberg states in a monolayer semiconductor, *Phys. Rev. Lett.* **120**, 057405 (2018).
- [38] J. Li, M. Goryca, N. P. Wilson, A. V. Stier, X. Xu, and S. A. Crooker, Spontaneous valley polarization of interacting carriers in a monolayer semiconductor, *Phys. Rev. Lett.* **125**, 147602 (2020).
- [39] E. Courtade, M. Semina, M. Manca, M. M. Glazov, C. Robert, F. Cadiz, G. Wang, T. Taniguchi, K. Watanabe, M. Pierre, W. Escoffier, E. L. Ivchenko, P. Renucci, X. Marie, T. Amand, and B. Urbaszek, Charged excitons in monolayer WSe<sub>2</sub>: Experiment and theory, *Phys. Rev. B* **96**, 085302 (2017).
- [40] A. Hichri and S. Jaziri, Trion fine structure and anomalous Hall effect in monolayer transition metal dichalcogenides, *Phys. Rev. B* **102**, 085407 (2020).
- [41] A. M. Jones, H. Yu, N. J. Ghimire, S. Wu, G. Aivazian, J. S. Ross, B. Zhao, J. Yan, D. G. Mandrus, D. Xiao, W. Yao, and X. Xu, Optical generation of excitonic valley coherence in monolayer WSe<sub>2</sub>, *Nat. Nanotechnol.* **8**, 634 (2013).
- [42] Z. Wang, J. Shan, and K. F. Mak, Valley- and spin-polarized Landau levels in monolayer WSe<sub>2</sub>, *Nat. Nanotechnol.* **12**, 144 (2017).
- [43] T. Wang, Z. Li, Z. Lu, Y. Li, S. Miao, Z. Lian, Y. Meng, M. Blei, T. Taniguchi, K. Watanabe, S. Tongay, W. Yao, D. Smirnov, C. Zhang, and S.-F. Shi, Observation of quantized exciton energies in monolayer WSe<sub>2</sub> under a strong magnetic field, *Phys. Rev. X* **10**, 021024 (2020).
- [44] T. Smoleński, O. Cotlet, A. Popert, P. Back, Y. Shimazaki, P. Knüppel, N. Dietler, T. Taniguchi, K. Watanabe, M. Kroner, and A. Imamoglu, Interaction-induced Shubnikov–de Haas oscillations in optical conductivity of monolayer MoSe<sub>2</sub>, *Phys. Rev. Lett.* **123**, 097403 (2019).
- [45] P. Kapuściński, D. Vaclavkova, M. Grzeszczyk, A. O. Slobodeniuk, K. Nogajewski, M. Bartos, K. Watanabe, T. Taniguchi, C. Faugeras, A. Babiński, M. Potemski, and M. R. Molas, Valley polarization of singlet and triplet trions in a WS<sub>2</sub> monolayer in magnetic fields, *Phys. Chem. Chem. Phys.* **22**, 19155-19161 (2020).
- [46] M. Zinkiewicz, T. Woźniak, T. Kazimierczuk, P. Kapuscinski, K. Oreszczuk, M. Grzeszczyk, M. Bartoš, K. Nogajewski, K. Watanabe, T. Taniguchi, C. Faugeras, P. Kossacki, M. Potemski, A. Babiński, and M. R. Molas, Excitonic complexes in n-doped WS<sub>2</sub> monolayer, *Nano Lett.* **21**, 2519 (2021).
- [47] J. Zipfel, K. Wagner, J. D. Ziegler, T. Taniguchi, K. Watanabe, M. A. Semina, and A. Chernikov, Light-matter coupling and non-equilibrium dynamics of exchange-split trions in monolayer WS<sub>2</sub>, *J. Chem. Phys.* **153**, 034706 (2020).
- [48] C. Robert, S. Park, F. Cadiz, L. Lombez, L. Ren, H. Tornatzky, A. Rowe, D. Paget, F. Sirotti, M. Yang, D. Van Tuan, T. Taniguchi, B. Urbaszek, K. Watanabe, T. Amand, H. Dery, and X. Marie, Spin/valley pumping of resident electrons in WSe<sub>2</sub> and WS<sub>2</sub> monolayers, *Nat. Commun.* **12**, 5455 (2021).
- [49] M. Goryca, J. Li, A. V. Stier, T. Taniguchi, K. Watanabe, E. Courtade, S. Shree, C. Robert, B. Urbaszek, X. Marie, and S. A. Crooker, Revealing exciton masses and dielectric properties of monolayer semiconductors with high magnetic fields, *Nat. Commun.* **10**, 4172 (2019).
- [50] G. Plechinger, P. Nagler, A. Arora, A. Granados del Aguila, M. V. Ballottin, T. Frank, P. Steinleitner, M. Gmitra, J. Fabian, P. C. M. Christianen, R. Bratschitsch, C. Schüller, and T. Korn, Excitonic valley effects in monolayer WS<sub>2</sub> under high magnetic fields, *Nano Lett.* **16**, 7899 (2016).
- [51] B. Scharf, D. van Tuan, I. Zutic, and H. Dery, Dynamical screening in monolayer transition-metal dichalcogenides and its manifestations in the exciton spectrum, *J. Phys.: Condens. Matter* **31**, 203001 (2019).
- [52] C. Robert, B. Han, P. Kapuscinski, A. Delhomme, C. Faugeras, T. Amand, M. R. Molas, M. Bartos, K. Watanabe, T. Taniguchi, B. Urbaszek, M. Potemski, and X. Marie, Measurement of the spin-forbidden dark excitons in MoS<sub>2</sub> and MoSe<sub>2</sub> monolayers, *Nat. Commun.* **11**, 4037 (2020).
- [53] S. Park, S. Arscott, T. Taniguchi, K. Watanabe, F. Sirotti, and F. Cadiz, Efficient valley polarization of charged excitons in Molybdenum disulfide monolayers by optical pumping, *Commun. Phys.* **5**, 73 (2022).
- [54] J. Klein, M. Florian, A. Hötger, A. Steinhoff, A. Delhomme, T. Taniguchi, K. Watanabe, F. Jahnke, A. W. Holleitner, M. Potemski, C. Faugeras, A. V. Stier, and J. J. Finley, Trions in MoS<sub>2</sub> are quantum superpositions of intra- and intervalley spin states, *Phys. Rev. B* **105**, L041302 (2022).
- [55] J. Klein, A. Hötger, M. Florian, A. Steinhoff, A. Delhomme, T. Taniguchi, K. Watanabe, F. Jahnke, A. W. Holleitner, M. Potemski, C. Faugeras, J. J. Finley, and A. V. Stier, Controlling exciton many-body states by the electric-field effect in monolayer MoS<sub>2</sub>, *Phys. Rev. Res.* **3**, L022009 (2021).
- [56] J. G. Roch, G. Froelicher, N. Leisgang, P. Makk, K. Watanabe, T. Taniguchi, and R. J. Warburton, Spin-polarized electrons in monolayer MoS<sub>2</sub>, *Nat. Nanotechnol.* **14**, 432 (2019).